tertiary phosphines.[12] On the basis of $Pt-P_{bridge}$ distances (average 2.348 Å) and Pt-P (terminal) distances (average 2.331 Å), they concluded that the two types of phosphorus substituents compete equally. In contrast to the nearly equal M-P bond distances found in the Pt complex, the two types of Rh-P bond distances differ significantly in the title compound: $Rh-P_{bridge}$, average 2.359 Å; $Rh-P_{terminal}$, average 2.256 Å. In terms of the relative bond-lengthening influences in the title compound, therefore, the bridging diphenylphosphido group would have to be considered to exert the weaker *trans*-directing influence.

The structural features as reported are fully consistent with predictions based on $^{31}P\{^1H\}$ NMR analysis.[5a,11] In substantiation of this structural report, we suggest that the observed $\delta_{P_{bridge}}$ resonance at -104 further demonstrates the lack of significant Rh-Rh bonding in this complex and of the utility of ^{31}P NMR spectroscopy for the structural characterization of transition-metal complexes that contain bridging organophosphido ligands.

Registry No. $[Rh(\mu\text{-}PPh_2)(DPPE)]_2 \cdot C_4H_8O$, 84332-81-0.

Supplementary Material Available: Listings of observed and calculated structure factor amplitudes, atom coordinates and isotropic thermal parameters, bond lengths, bond angles, and anisotropic thermal parameters (28 pages). Ordering information is given on any current masthead page.

Contribution from the Department of Chemistry, University of British Columbia, Vancouver, BC, Canada V6T 1Y6

Phosphine Complexes of Zirconium(IV) and Hafnium(IV) Obtained through the Use of Hybrid Multidentate Ligands. X-ray Crystal Structure of $ZrCl_2[N(SiMe_2CH_2PMe_2)_2]_2$

MICHAEL D. FRYZUK,* HUGH DAVID WILLIAMS, and STEVEN J. RETTIG

Received June 30, 1982

The reaction of $LiN(SiMe_2CH_2PR_2)_2$ with either $ZrCl_4$ or $HfCl_4$ generates new complexes of the formula $MCl_2[N(SiMe_2CH_2PR_2)_2]_2$ (M = Zr or Hf; R = Me or Ph). Both of the potentially tridentate hybrid ligands bind only in a bidentate fashion, generating coordinated and uncoordinated phosphines in the same molecule. The single-crystal X-ray structure of $ZrCl_2[N(SiMe_2CH_2PMe_2)_2]_2$ (space group *Pbca*; a = 16.8307 (9), b = 18.4663 (8), c = 24.285 (2) Å; Z = 8; R = 0.036 (R_w = 0.046)) indicates a distorted-octahedral geometry with trans chloride and cis phosphine ligands. The molecule is chiral both in the solid state and in solution by virtue of a "gear" effect of the two bulky disilylamide ligands.

Introduction

The chemistry of the group 4 metals, Ti, Zr, and Hf, is dominated by complexes containing the η^5-$C_5H_5^-$ or the η^5-$C_5Me_5^-$ ligand.[1] While these derivatives have established the unique reactivity patterns of these metals, new ligands and new combinations of ligands are currently being investigated to extend the potentially rich chemistry of this group.[2] One donor type that has only recently been incorporated into complexes of zirconium[2,4,5] and hafnium[6] is the *soft* phosphine ligand, PR_3 (R = aryl or alkyl). The evidence so far suggests that monodentate phosphine complexes of Zr(IV) are thermally labile[4] and subject to displacement by *hard* ligands such as NEt_3 or by chelating ligands. Clearly, mismatching the *soft* phosphine donors with the *hard* Zr(IV) and Hf(IV) centers is a major factor in this behavior. To overcome this mismatching of donors and acceptors, we have developed a new series of "hybrid" ligands[7] that incorporate the *soft* phosphine donor into a chelating array (Figure 1) that also contains the *hard* amido donor, $^-NR_2$ (R = alkyl, aryl, or silyl). Since amides of Zr(IV) and Hf(IV) are stable, well-known[8-10] complexes, we anticipated that the amide portion of the chelating ligand would serve as an *anchor* and reduce the tendency for phosphine dissociation. We present here full details of our initial work in this area, which has provided a new entry into phosphine derivatives of group 4B, specifically zirconium and hafnium.

Experimental Section

General Information. All manipulations were performed under prepurified nitrogen in a Vacuum Atmospheres HE-553-2 glovebox equipped with a MO-40-2H purification system or in standard Schlenk-type glassware. $ZrCl_4$ and $HfCl_4$ were obtained from Alfa and sublimed prior to use. Methylene chloride (CH_2Cl_2) was purified by distillation from CaH_2 under argon. Toluene, hexanes, and diethyl ether (Et_2O) were distilled from sodium-benzophenone ketyl under argon. Melting points were determined on a Mel-Temp apparatus in sealed capillaries under nitrogen and are uncorrected. Carbon, hydrogen, and nitrogen analyses were performed by Mr. P. Borda of this department. ^1H NMR spectra were recorded on one of the following instruments, depending on the complexity of the particular spectrum: Varian EM-360L, Bruker WP-80, Varian XL-100, or Bruker WH-400. $^{31}P\{^1H\}$ spectra were run at 32.442 MHz on the Bruker WP-80 in 10-mm tubes fitted with inserts for the internal standard $P(OMe)_3$ (set at +141.0 ppm relative to 85% H_3PO_4). Deuterated benzene (C_6D_6) and deuterated toluene (C_7D_8) were purchased from Aldrich, dried over activated 4-Å molecular sieves, and vacuum transferred prior to use. The starting ligand precursors $LiN(SiMe_2CH_2PR_2)_2$ (R = Ph[11b] or Me[12]) were prepared as described elsewhere.

$ZrCl_2[N(SiMe_2CH_2PPh_2)_2]_2$. A solution of $LiN(SiMe_2CH_2PPh_2)_2$ (8.56 g, 16.0 mmol) in Et_2O (150 mL) was added dropwise to a cold (-4 °C) suspension of $ZrCl_4$ (1.86 g, 8.0 mmol) in Et_2O (100 mL). The mixture was warmed to room temperature and stirred for 3 h. After the Et_2O was removed in vacuo, the residue was extracted with hexanes (2 × 20 mL) to remove the lemon yellow, "tris" derivative, $ZrCl[N(SiMe_2CH_2PPh_2)_2]_3$. Although this material was never ob-

(1) Labinger, J. A. *J. Organomet. Chem.* **1982**, *227*, 341.
(2) Reger, D. L.; Tarquini, M. E. *Inorg. Chem.* **1982**, *21*, 840.
(3) Gell, K. I.; Schwartz, J. *J. Chem. Soc., Chem. Commun.* **1979**, 245.
(4) Wengrovius, J. H.; Schrock, R. R. *J. Organomet. Chem.* **1981**, *205*, 319.
(5) Fischer, M. B.; James, E. J.; McNeese, T. J.; Nyburg, S. C.; Posin, B.; Wong-Ng, W.; Wreford, S. S. *J. Am. Chem. Soc.* **1980**, *102*, 4941.
(6) Wreford, S. S.; Whitney, J. F. *Inorg. Chem.* **1981**, *20*, 3918.
(7) Bertini, I.; Dapporta, P.; Fallani, G.; Sacconi, L. *Inorg. Chem.* **1971**, *10*, 1703 and references therein.
(8) Andersen, R. A. *Inorg. Chem.* **1979**, *18*, 1724, 2928.
(9) Lappert, M. F.; Power, P. P.; Sanger, A. R.; Srivastava, R. C. "Metal and Metalloid Amides"; Wiley: New York, 1979.
(10) Airoldi, C.; Bradley, D. C.; Chudzynska, H.; Hursthouse, M. B.; Malik, K. M. A.; Raithby, P. R. *J. Chem. Soc., Dalton Trans.* **1980**, 2010.
(11) (a) Fryzuk, M. D.; MacNeil, P. A. *J. Am. Chem. Soc.* **1981**, *103*, 3492. (b) Fryzuk, M. D.; MacNeil, P. A.; Secco, A. S.; Rettig, S. J.; Trotter, J. *Organometallics* **1982**, *1*, 918.
(12) Fryzuk, M. D.; Brzezowski, C.; MacNeil, P. A.; Williams, H. D., manuscript in preparation.

0020-1669/83/1322-0863$01.50/0

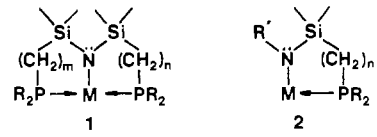

1 2

Figure 1. Hybrid tridentate (**1**) and bidentate (**2**) ligands (M is a transition metal).

Table I. Crystal Data and Experimental Conditions for Data Collection

$C_{20}H_{56}Cl_2N_2P_4Si_4Zr$	fw 723.05
$a = 16.8307$ (9) Å	space group *Pbca*
$b = 18.4663$ (8) Å	$Z = 8$
$c = 24.285$ (2) Å	$V = 7547.8$ (8) Å^3
$\mu = 6.68$ cm^{-1}	$D_c = 1.273$ g cm^{-3}

radiation: Mo Kα, graphite monochromator, $2\theta = 12.2°$, $\lambda = 0.71073$ Å
scan: ω-2θ, range $(0.65 + 0.35 \tan \theta)°$ in ω, extended 25% on each side for bkgds, speed 0.7–10.1° min^{-1} to give $I/\sigma(I) \geq 28.6$
aperture: $(2.0 + \tan \theta) \times 4$ mm, 173 mm from cryst
stds: reflectns 0,12,5, 587, 10,8,1 monitored every hour of exposure time, random intens fluctuations of ±2% (three reflctns recentered every 150 reflctns for orientation control)
data collected: h,k,l for $0 < 2\theta < 55°$
$\sigma^2(I)$: $S + 2B + [0.04(S - B)]^2$ (S = scan count, B = bkgd count)
boundary planes: 6 faces; {001}, (111), (−1,−1,1), (−1,1,1), (1,−1,1)
transmission factors: 0.675–0.889
cryst size: ca. 0.48 × 0.50 × 0.50 mm
temp: 21 ± 1 °C

tained analytically pure, its spectral properties[13] are consistent with this formulation. The hexanes-insoluble residue was extracted with toluene (3 × 30 mL); the toluene solution was filtered through Celite and concentrated to ~30 mL and hexanes was added to give the product as colorless crystals, yield 5.8 g (60%). Recrystallization from CH_2Cl_2 and hexanes gave colorless prisms that contain $^1/_2$ equiv of CH_2Cl_2 of crystallization (confirmed by ^{1}H NMR); mp 228–230 °C. Anal. Calcd for $C_{60.5}H_{73}Cl_3N_2P_4Si_4Zr$: C, 57.60; H, 5.83; N, 2.22. Found: C, 57.87; H, 5.96; N, 2.26.

$HfCl_2[N(SiMe_2CH_2PPh_2)_2]_2$. The procedure follows that of the zirconium derivative except that the initial Et_2O solution was stirred for 4 h at room temperature to give the product in 50% yield. Recrystallization from CH_2Cl_2 and hexanes gave colorless crystals that contain one CH_2Cl_2 of crystallization (confirmed by ^{1}H NMR); mp 238–243 °C. Anal. Calcd for $C_{61}H_{74}Cl_4HfN_2P_4Si_4$: C, 52.05; H, 5.30; N, 1.99; Cl, 10.07. Found: C, 51.76; H, 5.33; N, 1.85; Cl, 10.03.

$ZrCl_2[N(SiMe_2CH_2PMe_2)_2]_2$. A solution of $LiN(SiMe_2CH_2PMe_2)_2$ (1.04 g, 3.62 mmol) in hexanes (30 mL) was added dropwise to a cold (−4 °C) suspension of $ZrCl_4$ (0.421, 1.81 mmol) in Et_2O (50 mL). The reaction mixture was warmed to room temperature and stirred for 2.5 h, at which time the Et_2O was removed in vacuo. Extraction with hexanes (4 × 20 mL) followed by filtration and concentration gave the product as a white solid. Recrystallization from minimum hexanes gave colorless prisms: yield 0.790 g (60%); mp 134–136 °C. Anal. Calcd for $C_{20}H_{56}Cl_2N_2P_4Si_4Zr$: C, 33.22; H, 7.81; N, 3.87. Found: C, 33.67; H, 8.18; N, 3.20.

$HfCl_2[N(SiMe_2CH_2PMe_2)_2]_2$. The compound was prepared by the exact procedure used for the zirconium analogue: yield 65%; mp 137–138 °C. Anal. Calcd for $C_{20}H_{56}Cl_2HfN_2P_4Si_4$: C, 29.64; H, 6.96; N, 3.46. Found: C, 29.90; H, 6.84; N, 3.59.

X-ray Crystallographic Analysis of $ZrCl_2[N(SiMe_2CH_2PMe_2)_2]_2$ (4b). A colorless crystal of **4b** was sealed under dry nitrogen in a Lindemann glass capillary tube and mounted on an Enraf-Nonius CAD4-F diffractometer in a nonspecific orientation. Final unit cell parameters were determined by least squares on 2 $(\sin \theta)/\lambda$ values for 25 reflections (with $35 < 2\theta < 43°$) measured with Mo $K\alpha_1$ radiation ($\lambda = 0.70930$ Å). Crystal data and conditions for data collection are summarized in Table I. Of 8615 independent reflections (with $2\theta \leq 55°$) measured, 4069 had $I > 3\sigma(I)$ and were employed in the structure solution and refinement. The computer programs employed have been described previously.[14]

Table II. Final Positional (Fractional ×10^5, C ×10^4) and Isotropic Thermal Parameters ($U \times 10^3$ Å^2) with Estimated Standard Deviations in Parentheses

atom	x	y	z	U_{eq}/ U_{iso}
Zr	55039 (2)	10231 (2)	63998 (2)	42
Cl(1)	67135 (6)	9029 (6)	69600 (5)	60
Cl(2)	45781 (7)	7014 (6)	56544 (5)	60
P(1)	54661 (8)	−4906 (6)	64806 (5)	55
P(2)	54013 (9)	11672 (8)	89018 (6)	71
P(3)	66742 (7)	8282 (7)	55977 (6)	59
P(4)	30772 (10)	29293 (11)	61396 (9)	102
Si(1)	40059 (7)	1608 (7)	70427 (6)	54
Si(2)	48337 (8)	13489 (7)	76674 (6)	54
Si(3)	66447 (8)	23983 (7)	59653 (6)	60
Si(4)	48820 (8)	26480 (7)	59573 (6)	62
N(1)	47205 (19)	8514 (18)	70577 (15)	47
N(2)	56929 (19)	20814 (18)	61166 (15)	48
C(1)	4415 (3)	−607 (2)	6614 (2)	63
C(2)	5396 (3)	809 (3)	8195 (2)	60
C(3)	7288 (3)	1602 (3)	5765 (2)	60
C(4)	3948 (3)	2365 (3)	6317 (3)	76
C(5)	5700 (4)	−1158 (3)	5950 (2)	81
C(6)	5943 (3)	−863 (3)	7091 (2)	72
C(7)	6129 (4)	566 (4)	9219 (2)	90
C(8)	4503 (4)	738 (4)	9179 (3)	89
C(9)	7356 (4)	70 (4)	5533 (3)	110
C(10)	6383 (4)	994 (3)	4896 (2)	93
C(11)	2268 (5)	2369 (6)	6311 (7)	256
C(12)	2997 (9)	3425 (9)	6705 (6)	286
C(13)	3754 (3)	−250 (3)	7724 (2)	82
C(14)	3054 (3)	476 (3)	6737 (2)	72
C(15)	5420 (3)	2203 (3)	7569 (2)	72
C(16)	3851 (3)	1671 (3)	7935 (2)	75
C(17)	6714 (4)	3029 (3)	5365 (3)	99
C(18)	7106 (3)	2862 (3)	6566 (3)	78
C(19)	4660 (4)	2636 (3)	5206 (3)	86
C(20)	5078 (4)	3598 (3)	6187 (3)	99

The coordinates of the Zr, Cl, and P, and Si atoms were determined from the Patterson function and those of the remaining non-hydrogen atoms from a subsequent difference map. Refinement was full-matrix least squares, with minimization of $\sum w(|F_o| - |F_c|)^2$, where $w = 1/\sigma^2(F)$. Neutral-atom scattering factors and anomalous dispersion corrections (employed for Zr, Cl, P, and Si atoms) were taken from ref 15. Refinement of the non-hydrogen atoms with anisotropic thermal parameters resulted in $R = \sum(||F_o| - |F_c||)/\sum|F_o| = 0.052$ and $R_w = [\sum w(|F_o| - |F_c|)^2/\sum w(F_o)^2]^{1/2} = 0.080$. A difference map at this point revealed 50 of the 56 hydrogen atoms, those not located being associated with C(11) and C(12), which, in view of their large thermal parameters, are probably disordered. No attempt to resolve this rotational disorder about the P(4)–C(4) bond was made, the uncoordinated $P(4)Me_2$ moiety not being an important part of the structure; the ordered model was retained. Contributions to the structure factors of the 56 H atoms were included in the calculations with use of "ideal" positional parameters (C–H = 0.98 Å) and isotropic thermal parameters ($U_H = U_C + 0.011$ Å^2), recalculated after each cycle of refinement.

Convergence was reached at $R = 0.036$ and $R_w = 0.046$ for 4069 reflections and 298 variables. The mean error in an observation of unit weight was 1.807 e. The mean and maximum parameter shifts on the final cycle of refinement corresponded to 0.05σ and 0.85σ, the largest shift being associated with the U_{22} parameter of C(12). A final difference map revealed, not unexpectedly, four peaks in the range 0.5–0.75 e Å^{-3} in the vicinity of the $P(4)Me_2$ group, indicating that the ordered model is not ideal but satisfactorily accounts for the electron density in this region. No other unusual features were noted; the largest residual peaks on the remainder of the difference map were 0.35 e Å^{-3} near the Zr and Cl atoms. Final positional and equivalent

(13) $ZrCl[N(SiMe_2CH_2PPh_2)_2]_3$ ^{1}H NMR (C_6D_6, ppm): $Si(CH_3)_2$, 0.02 (s); PCH_2Si, 1.27 (br s); $P(C_6H_5)_2$, 7.10 (m, meta/para), 7.50 (m, ortho).

(14) Ball, R. G.; Hames, B. W.; Legzdins, P.; Trotter, J. *Inorg. Chem.* **1980**, *19*, 3626.

(15) "International Tables for X-Ray Crystallography"; Kynoch Press: Birmingham, England, 1974; Vol. IV, pp 99, 149.

Table VI. Bond Lengths (Å) with Estimated Standard Deviations in Parentheses

atoms	length	atoms	length
Zr-Cl(1)	2.4585 (11)	P(4)-C(12)	1.657 (11)
Zr-Cl(2)	2.4613 (12)	Si(1)-N(1)	1.753 (3)
Zr-P(1)	2.8028 (12)	Si(1)-C(1)	1.890 (5)
Zr-P(3)	2.7936 (13)	Si(1)-C(13)	1.869 (5)
Zr-N(1)	2.096 (4)	Si(1)-C(14)	1.859 (5)
Zr-N(2)	2.096 (3)	Si(2)-N(1)	1.753 (4)
P(1)-C(1)	1.811 (5)	Si(2)-C(2)	1.880 (5)
P(1)-C(5)	1.826 (5)	Si(2)-C(15)	1.875 (5)
P(1)-C(6)	1.821 (5)	Si(2)-C(16)	1.873 (5)
P(2)-C(2)	1.839 (5)	Si(3)-N(2)	1.745 (3)
P(2)-C(7)	1.823 (6)	Si(3)-C(3)	1.890 (5)
P(2)-C(8)	1.835 (6)	Si(3)-C(17)	1.870 (6)
P(3)-C(3)	1.809 (5)	Si(3)-C(18)	1.862 (5)
P(3)-C(9)	1.817 (6)	Si(4)-N(2)	1.763 (4)
P(3)-C(10)	1.799 (6)	Si(4)-C(4)	1.872 (6)
P(4)-C(4)	1.849 (5)	Si(4)-C(19)	1.862 (6)
P(4)-C(11)	1.761 (10)	Si(4)-C(20)	1.870 (6)

Table VII. Bond Angles (deg) with Estimated Standard Deviations in Parentheses

atoms	angle	atoms	angle
Cl(1)-Zr-Cl(2)	155.42 (4)	N(1)-Si(1)-C(13)	115.6 (2)
Cl(1)-Zr-P(1)	83.69 (4)	N(1)-Si(1)-C(14)	111.8 (2)
Cl(1)-Zr-P(3)	77.90 (4)	C(1)-Si(1)-C(13)	105.4 (2)
Cl(1)-Zr-N(1)	94.91 (10)	C(1)-Si(1)-C(14)	109.3 (2)
Cl(1)-Zr-N(2)	98.06 (10)	C(13)-Si(1)-C(14)	106.5 (3)
Cl(2)-Zr-P(1)	78.25 (4)	N(1)-Si(2)-C(2)	110.6 (2)
Cl(2)-Zr-P(3)	84.40 (4)	N(1)-Si(2)-C(15)	113.0 (2)
Cl(2)-Zr-N(1)	97.23 (10)	N(1)-Si(2)-C(16)	111.3 (2)
Cl(2)-Zr-N(2)	94.57 (10)	C(2)-Si(2)-C(15)	105.5 (2)
P(1)-Zr-P(3)	86.35 (4)	C(2)-Si(2)-C(16)	112.1 (2)
P(1)-Zr-N(1)	77.38 (10)	C(15)-Si(2)-C(16)	104.0 (2)
P(1)-Zr-N(2)	162.99 (11)	N(2)-Si(3)-C(3)	108.6 (2)
P(3)-Zr-N(1)	162.90 (10)	N(2)-Si(3)-C(17)	115.5 (2)
P(3)-Zr-N(2)	77.55 (10)	N(2)-Si(3)-C(18)	111.8 (2)
N(1)-Zr-N(2)	119.12 (14)	C(3)-Si(3)-C(17)	104.4 (3)
Zr-P(1)-C(1)	98.83 (15)	C(3)-Si(3)-C(18)	108.7 (2)
Zr-P(1)-C(5)	128.3 (2)	C(17)-Si(3)-C(18)	107.4 (3)
Zr-P(1)-C(6)	115.1 (2)	N(2)-Si(4)-C(4)	112.4 (2)
C(1)-P(1)-C(5)	104.8 (3)	N(2)-Si(4)-C(19)	111.3 (2)
C(1)-P(1)-C(6)	103.9 (2)	N(2)-Si(4)-C(20)	110.8 (2)
C(5)-P(1)-C(6)	102.9 (3)	C(4)-Si(4)-C(19)	106.5 (3)
C(2)-P(2)-C(7)	100.3 (2)	C(4)-Si(4)-C(20)	105.7 (3)
C(2)-P(2)-C(8)	100.5 (3)	C(19)-Si(4)-C(20)	109.8 (3)
C(7)-P(2)-C(8)	97.8 (3)	Zr-N(1)-Si(1)	121.7 (2)
Zr-P(3)-C(3)	98.3 (2)	Zr-N(1)-Si(2)	119.8 (2)
Zr-P(3)-C(9)	127.2 (2)	Si(1)-N(1)-Si(2)	118.2 (2)
Zr-P(3)-C(10)	116.5 (2)	Zr-N(2)-Si(3)	121.4 (2)
C(3)-P(3)-C(9)	105.5 (3)	Zr-N(2)-Si(4)	120.5 (2)
C(3)-P(3)-C(10)	103.5 (2)	Si(3)-N(2)-Si(4)	117.7 (2)
C(9)-P(3)-C(10)	102.8 (3)	P(1)-C(1)-Si(1)	111.4 (2)
C(4)-P(4)-C(11)	103.1 (4)	P(2)-C(2)-Si(2)	116.6 (3)
C(4)-P(4)-C(12)	100.6 (5)	P(3)-C(3)-Si(3)	110.2 (2)
C(11)-P(4)-C(12)	93.8 (9)	P(4)-C(4)-Si(4)	113.6 (3)
N(1)-Si(1)-C(1)	107.9 (2)		

isotropic thermal parameters (U_{eq} = $^1/_3$(trace U)) for the non-hydrogen atoms are listed in Table II and calculated coordinates and isotropic thermal parameters for the hydrogen atoms in Table III. Anisotropic thermal parameters are given in Table IV and observed and calculated structure factor amplitudes in Table V. Bond lengths and angles for the non-hydrogen atoms and intraannular torsion angles for the two chelate rings appear in Tables VI, VII, and VIII, respectively, and a complete listing of torsion angles is given in Table IX. Tables III–V and IX appear in the supplementary material.

Results and Discussion

Synthesis of $MCl_2[N(SiMe_2CH_2PR_2)_2]_2$ Derivatives. We have previously[11] used the lithium amide $LiN(SiMe_2CH_2PPh_2)_2$ (**3a**) as a convenient reagent to a potentially tridentate "hybrid" ligand of the type **1** ($m = n = 1$ in Figure 1) with the metals of the nickel triad. This procedure also works well for the group 4B metal halides $ZrCl_4$ and $HfCl_4$.

Table VIII. Intraannular Torsion Angles (deg) with Standard Deviations in Parentheses

atoms	angle
N(1)-Zr-P(1)-C(1)	40.3 (2)
Zr-P(1)-C(1)-Si(1)	−34.5 (2)
N(1)-Si(1)-C(1)-P(1)	12.4 (3)
C(1)-Si(1)-N(1)-Zr	30.5 (3)
P(1)-Zr-N(1)-Si(1)	−41.2 (2)
N(2)-Zr-P(3)-C(3)	42.0 (2)
Zr-P(3)-C(3)-Si(3)	−37.9 (2)
N(2)-Si(3)-C(3)-P(3)	16.7 (3)
C(3)-Si(3)-N(2)-Zr	27.0 (3)
P(3)-Zr-N(2)-Si(3)	−40.0 (2)

Table X. $^{31}P\{^1H\}$ Data[a] for the $MCl_2[N(SiMe_2CH_2PR_2)_2]_2$ Derivatives

no.	compd	^{31}P chem shift, ppm[a]
3a	$LiN(SiMe_2CH_2PPh_2)_2$[b]	−23.2 (br s)
3b	$LiN(SiMe_2CH_2PMe_2)_2$[c]	−56.2 (br s)
4a	$ZrCl_2[N(SiMe_2CH_2PPh_2)_2]_2$	−12.7 (s), −19.8 (s)
4b	$ZrCl_2[N(SiMe_2CH_2PMe_2)_2]_2$	−30.7 (s), −52.6 (s)
5a	$HfCl_2[N(SiMe_2CH_2PPh_2)_2]_2$	−10.6 (s), −19.6 (s)
5b	$HfCl_2[N(SiMe_2CH_2PMe_2)_2]_2$	−30.8 (s), −53.1 (s)

[a] All chemical shifts are relative to $P(OMe)_3$ at +141.0 ppm. [b] Reference 11b. [c] Reference 12.

Thus the metathesis of **3a** with either $ZrCl_4$ or $HfCl_4$ in diethyl ether produces new compounds of the stoichiometry $MCl_2[N(SiMe_2CH_2PPh_2)_2]_2$ (M = Zr, **4a**; M = Hf, **5a**). If less than 2 equiv of **3a** is used, the yields of **4a** and **5a** are decreased; recrystallized yields are generally 60% or better if 2 equiv of **3a** is utilized. A variable amount of a lemon yellow side product is observed in these reactions; increasing the stoichiometry of **3a** to greater than 3 equiv increases the yield of this side product. We believe this material to be the "tris" derivative $MCl[N(SiMe_2CH_2PPh_2)_2]_3$; however, an analytically pure product could not be obtained. The corresponding reaction with the monodentate amide precursor, $LiN(SiMe_3)_2$, generates both the "bis" derivatives $MCl_2[N(SiMe_3)_2]_2$ and the "tris" derivatives $MCl[N(SiMe_3)_2]_3$ by control of stoichiometry and temperature.[8,10]

The corresponding hybrid ligand precursor, $LiN(SiMe_2CH_2PMe_2)_2$[12] (**3b**), which contains the dimethylphosphine donors, can be used in a completely analogous reaction (eq 1) to produce the "bis" derivatives $MCl_2[N(SiMe_2CH_2PMe_2)_2]_2$ (M = Zr, **4b**; M = Hf, **5b**). Regardless of the stoichiometry used in the reaction of **3b** (1–3 equiv) with either $ZrCl_4$ or $HfCl_4$, only the "bis" derivatives are produced with no evidence of any side products as is observed with **3a**.

$$MCl_4 + 2LiN(SiMe_2CH_2PR_2)_2 \xrightarrow{Et_2O} MCl_2[N(SiMe_2CH_2PR_2)_2]_2 + 2LiCl \quad (1)$$

4a, M = Zr, R = Ph
4b, M = Zr, R = Me
5a, M = Hf, R = Ph
5b, M = Hf, R = Me

All of these new zirconium and hafnium derivatives are obtained as colorless, air- and moisture-sensitive, crystalline solids. Although these complexes are soluble in aromatic solvents, only the dimethylphosphino-substituted derivatives, **4b** and **5b**, show appreciable solubility in hexanes.

The proton-decoupled ^{31}P NMR spectra for these compounds all show similar features; each consists of two sharp singlets corresponding to both coordinated and uncoordinated phosphorus nuclei in the same molecule (Table X). For example, the $^{31}P\{^1H\}$ spectrum of $ZrCl_2[N(SiMe_2CH_2PPh_2)_2]_2$ (**4a**) displays two singlets of equal intensity at −12.7 and −19.8 ppm due to, respectively, coordinated phosphine and uncoordinated phosphine; we cannot account for the small differ-

Table XI. 400-MHz ^{1}H NMR Data[a] for the $MCl_2[N(SiMe_2CH_2PR_2)_2]_2$ Derivatives

		coord		uncoord		
no.	compd	$Si(CH_3)_2$	PCH_2Si	$Si(CH_3)_2$	PCH_2Si	other
4a	$ZrCl_2[N(SiMe_2CH_2PPh_2)_2]_2$	0.10 (s)	1.40 (m)	0.35 (br s)	1.50 (br d, J = 14)	$P(C_6H_5)_2$ 6.90 (m), 7.20 (m),
		0.62 (s)	2.77 (m)	0.80 (br s)	2.21 (d)	7.30 (br m), 7.60 (m), 7.74 (m)
4b	$ZrCl_2[N(SiMe_2CH_2PMe_2)_2]_2$	0.34 (s)	0.57 (m)	0.77 (br s)	1.30 (br s)	$P(CH_3)_2$[b] 0.92 (m), 1.15 (d, J_P = 3)
		0.63 (s)	1.83 (m)	0.80 (br s)	1.32 (br s)	
5a	$HfCl_2[N(SiMe_2CH_2PPh_2)_2]_2$	0.18 (s)	1.40 (m)	0.40 (br s)	1.50 (br d, J = 14)	$P(C_6H_5)_2$ 6.80 (m), 7.20 (m),
		0.65 (s)	2.70 (m)	0.80 (br s)	2.20 (d)	7.30 (br m), 7.60 (m), 7.71 (m)
5b	$HfCl_2[N(SiMe_2CH_2PMe_2)_2]_2$	0.28 (s)	0.48 (m)	0.68 (br s)	1.30 (br s)	$P(CH_3)_2$[b] 0.83 (m), 1.07 (d, J_P = 3)
		0.55 (s)	1.60 (m)	0.72 (br s)	1.33 (br s)	

[a] All spectra were recorded in C_6D_6. Chemical shifts are referenced to C_6D_5H at 7.15 ppm. All coupling constants are given in hertz. [b] The upfield multiplet corresponds to half of the coordinated phosphorus methyl protons, the other half being coincident with the doublet to lower field of the uncoordinated phosphorus methyl protons.

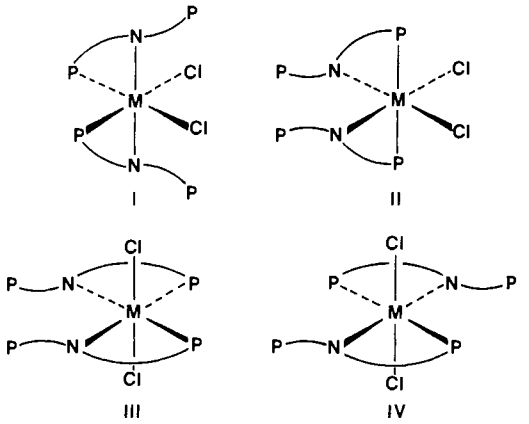

Figure 2. Four possible stereoisomeric structures for the derivatives $MCl_2[N(SiMe_2CH_2PR_2)_2]_2$ (M = Zr or Hf; R = Ph or Me).

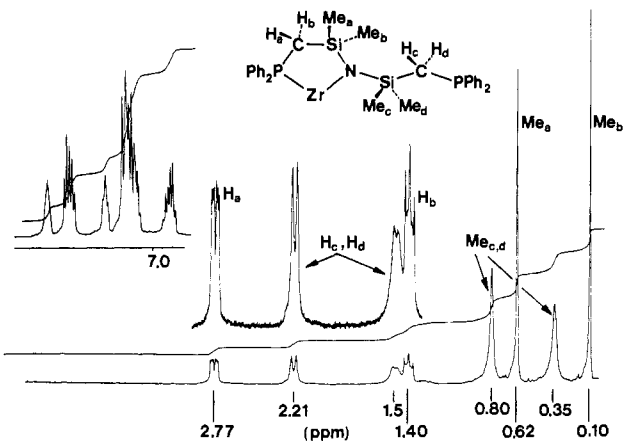

Figure 3. 400-MHz ^{1}H NMR spectrum of $ZrCl_2[N(SiMe_2CH_2PPh_2)_2]_2$ (**4a**).

ences in chemical shifts (3.1–3.6 ppm) between the dangling phosphines of **4** and **5** and the free[16] phosphines of the lithium amides **3a** and **3b**. The $^{31}P\{^1H\}$ spectra of the new zirconium and hafnium complexes are temperature independent between −80 and +60 °C except for a broadening and subsequent sharpening of the singlet due to free phosphine as the temperature is lowered.

With the assumption of a bidentate[17] mode of ligation for each ligand, four stereoisomeric structures (excluding enantiomers), all having a $MCl_2N_2P_2$ core (M = Zr or Hf) and octahedral geometry, can be envisioned (Figure 2). Further refinement of the solution structures can be made by analysis of the ^{1}H NMR spectra (Table XI). The ^{1}H NMR spectrum of **4a** (Figure 3) is typical: the silylmethyl protons appear as four alternating broad and sharp singlets at 0.80, 0.62, 0.35, and 0.10 ppm, while the methylene ($SiCH_2P$) protons appear as four multiplets at 2.77, 2.21, 1.50, and 1.40 ppm. Homonuclear and heteronuclear (^{31}P) decoupling experiments establish that the resonances at 2.77 and 1.40 ppm are due to the methylene protons adjacent to the *coordinated* phosphine. This pattern can be simulated[18] as a AA'MM'XX' spin system with a phosphorus–phosphorus coupling ($^2J_{XX'}$) in the range characteristic of cis-disposed phosphine donors.[19] This therefore excludes structures II and IV in Figure 2 since they require trans phosphine donors. Structure I appears to fit the data best as it is a chiral molecule (C_2 symmetry), which therefore renders the silylmethyl groups and the methylene protons diastereotopic by symmetry. The ^{1}H NMR spectrum of the related zirconium complex, **4b**, which has PMe_2 donors, is consistent with structure I as well, although there are differences in the resonances of the dangling portion of the phosphine ligand (Table XI). Very little change in chemical shifts or coupling constants is observed when hafnium is substituted for zirconium. Variable-temperature ^{1}H NMR studies on these compounds show that the chelated portion of the ligand is quite rigid between −80 and +60 °C; higher temperatures cause broadening and decomposition. The dangling portion of the ligand, however, is quite floppy since broadening is observed at lower temperatures; this broadening parallels the $^{31}P\{^1H\}$ results and may be due to conformational changes in the free portion of the ligands.

Molecular Structure of $ZrCl_2[N(SiMe_2CH_2PMe_2)_2]_2$ (4b). To accurately elucidate the molecular architecture of this complex, we have subjected crystals of **4b**, $ZrCl_2[N(SiMe_2CH_2PMe_2)_2]_2$, to X-ray analysis. The solid-state structure is shown in Figure 4. To our surprise the geometry corresponds to stereoisomer III and not the predicted isomeric structure I. Thus the structure can be described as distorted octahedral with trans chloride and cis amide donors. This particular geometry was initially rejected for the following reasons: (i) generally speaking, *trans*-[M(bidentate)$_2$(unidentate)$_2$] type complexes are not chiral; (ii) intuitively, the bulky disilylamide donors should prefer a trans disposition to minimize steric interactions. However, examination of the structure in Figure 4 reveals near-C_2 symmetry (and is therefore chiral, both enantiomers being present in the solid) by virtue of a "gear" effect whereby the bulky, dangling $SiMe_2CH_2PMe_2$ groups are locked above and below the ZrN_2P_2 plane. The two dangling PMe_2 groups are not sym-

(16) (a) We have been unable to detect any interaction[16b] between the phosphine donors and the lithium atom by either ^{1}P or ^{7}Li NMR experiments.[12] (b) Colquhoun, I. J.; McFarlane, H. C. E.; McFarlane, W. *J. Chem. Soc., Chem. Commun.* **1982**, 220.

(17) Other stereoisomers with tridentate–monodentate ligand combinations are easily excluded on the basis of ^{1}H NMR (Table XI).

(18) Simulations of NMR spin systems were performed with use of the PANIC program available on the Bruker NMR instruments.

(19) The following coupling constants were obtained from the simulation: J_{AM} = 14.0 Hz; $J_{AX'}$ = 2.00 Hz; J_{AX} = 8.00 Hz; J_{MX} = 15.0 Hz; $J_{XX'}$ = 35.0 Hz. All other undefined coupling constants are equal to zero. Trans phosphines normally generate "virtually" coupled spin systems. See: Brookes, P. R.; Shaw, B. L. *J. Chem. Soc. A*, **1967**, 1079.

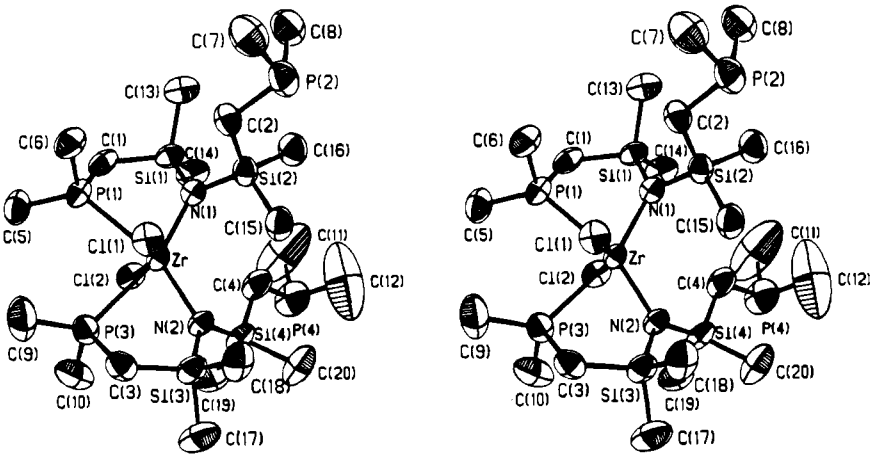

Figure 4. Stereoscopic view and atom-labeling scheme for $ZrCl_2[N(SiMe_2CH_2PMe_2)_2]_2$ (**4b**).

metrically disposed, breaking the C_2 symmetry exhibited by the remainder of the molecule. The two five-membered chelate rings, each having a distorted Zr-envelope conformation, are joined at the metal atom to generate a chairlike "step" arrangement: the backbone of the chelate ring defined by ZrN(1)P(1) is directed toward Cl(2) while that of the second ring is directed toward Cl(1). The anticipated nonbonding repulsions between the bulky disilylamide donors is reduced not only by this "gear" effect but also by an opening of the N–Zr–N angle from the idealized octahedral value of 90° to the observed 119.12 (14)°; in addition, the Cl–Zr–Cl angle closes to 155.42 (4)° away from the bulky silylamides.

The Zr–P bond distances of 2.803 (1) and 2.794 (1) Å are in good agreement with the Zr–P distances of 2.730 (4)–2.805 (4) Å observed in the formally Zr(II) derivative $ZrH(\eta^5\text{-}C_8H_{11})(Me_2PCH_2CH_2PMe_2)_2$.[5] The mean Zr–N and Zr–Cl distances in **4b** of 2.096 (1) and 2.460 (1) Å, respectively, may be compared to corresponding values of 2.070 (3) and 2.394 (2) Å in the tetrahedral complex $ZrCl[N(SiMe_3)_2]_3$.[10] The Zr–Cl distances in the title compound are more similar to those observed in molecules such as $(\eta^5\text{-}C_5H_5)_2ZrCl_2$, where the average Zr–Cl distance is 2.44 (1) Å.[20]

The coordination geometry of **4** is remarkably similar to that of $UCl_2[N(SiMe_3)_2]_2(MeOCH_2CH_2OMe)$;[21] this uranium(IV) derivative also has a distorted-octahedral geometry with trans chloride and cis silylamide ligands with an opened N–U–N bond angle of 122.7 (3)°. This particular geometry has been rationalized with use of Kepert's point-on-a-sphere model;[22] however, the structure of **4b** cannot be similarily treated since Kepert's model requires that the bidentate ligands have identical donor atoms for the normalized bite, *b* (defined as the distance between the chelating donor atoms divided by the metal to donor atom distance) to be calculated.[23]

The mean Si–N, Si–C, and P–C distances in the chelate rings of **4b** (1.749 (4), 1.890 (1), and 1.810 (1) Å, respectively) may be compared to the corresponding mean values of 1.714 (3), 1.887 (3), and 1.811 (5) Å observed in the related compounds $[MClN(SiMe_2CH_2PPh_2)_2]$ (M = Ni, Pd) and $[NiCl_2NH(SiMe_2CH_2PPh_2)_2]$.[11b] The longer Si–N distances in **4b** as compared to those in the nickel and palladium amides probably reflect the extent to which the nitrogen lone pair is delocalized into either empty metal d orbitals or silicon d orbitals. As noted previously,[11b] the Si–C and P–C bonds in the chelate rings are longer and shorter, respectively, than expected and suggest some degree of bond strength alternation in the N–Si–C–P–Zr fragments. The Si–C and P–C distances in the uncoordinated portion of the ligand (1.876 (4) and 1.845 (6) Å) are nearer the expected values of 1.865 and 1.840 Å. The nitrogen atoms are nearly planar, being displaced from the Si_2Zr planes by an average of 0.058 (2) Å.

With the exception of a weak C–H···Cl interaction [Cl(2)···H(10c) ($1-x, -y, 1-z$): Cl···H = 2.83, Cl···C = 3.770 (6) Å, C–H···Cl = 162°], all intermolecular distances correspond to normal van der Waals contacts. There are also three *intramolecular* Cl···H distances in the range 2.81–2.86 Å (between Cl(1) and protons attached to C(3) and C(15) and between Cl(2) and the C(4) methylene group). The corresponding Cl···C distances range from 3.319 (2) to 3.626 (5) Å and the C–H···Cl angles from 109 to 138°; however, Zr–Cl···H angles of 75–90° are not consistent with conventional hydrogen bonding.[24]

Reaction Chemistry of the $MCl_2[N(SiMe_2CH_2PR_2)_2]_2$ Complexes. Central to the design of these multidentate ligands is their ability to withstand substitution of the *soft* phosphine donors by other ligands, specifically *hard* ligands. Indeed, the addition of THF, NEt_3, pyridine, or TMEDA (typical *hard* neutral ligands) does not affect the overall ^1H and $^{31}P\{^1H\}$ NMR characteristics of these complexes, thus providing good evidence that our design strategy works, at least for five-membered chelate rings.

The rich chemistry of the group 4B metals is concerned with transformations involving metal–hydride or metal–alkyl bonds.[25] Disappointingly, all of our attempts to generate metal alkyls or metal hydrides by displacement of the chloride ligands have failed. For instance, the reaction of simple Grignard reagents such as methylmagnesium chloride (MeMgCl) in ether with either **4** or **5** resulted in the isolation of only starting materials; similar results with alkyllithium derivatives were observed. Metathesis type reactions with $LiBH_4$[8] or Me_3SiCN[11b] were also ineffective, with the zirconium or hafnium starting complexes being recovered in nearly quantitative yield. Lithium triethylborohydride ($LiEt_3BH$) also failed to displace the chloride ligands. The reaction of $AgBF_4$ in THF with **4a** and **4b** does generate a white precipitate, presumably AgCl; however, we have been unable to characterize the residue.

(20) Prout, C. K.; Cameron, T. S.; Forder, R. A.; Critchley, S. R.; Denton, B.; Rees, G. V.; *Acta Crystallogr., Sect. B* **1974**, *B30*, 2290.
(21) McCullough, L. G.; Turner, H. W.; Andersen, R. A.; Zalkin, A.; Templeton, D. H. *Inorg. Chem.* **1981**, *20*, 2869.
(22) Kepert, D. L. *Prog. Inorg. Chem.* **1977**, *23*, 1.
(23) Extending Kepert's model by defining an "averaged" normalized bite, b_{av}, as the distance between the donor atoms divided by the average metal to donor atom distance gives a value of 1.26, which does predict a trans geometry for complexes of the type $[M(bidentate)_2(unidentate)_2]$.
(24) Cotton, F. A.; Wilkinson, G. "Advanced Inorganic Chemistry", 4th ed.; Wiley: New York, 1980; p 223.
(25) Manriquez, J. M.; McAlister, D. R.; Sanner, R. D.; Bercaw, J. E. *J. Am. Chem. Soc.* **1978**, *100*, 2716.

We believe that the inertness of these complexes to further modification is a function of both the steric constraints that the ligand imparts on the metal derivative and an electronic effect. From the X-ray structure of the zirconium derivative **4b**, both the chloride ligands are surrounded by bulky $SiMe_2$ or PMe_2 groups, which can shield the Zr–Cl (or Hf–Cl) bonds from incoming nucleophilic reagents. In addition, the electronic effect of the weak C–H···Cl interactions may further reduce the tendency for substitution.

Conclusion

Our strategy in the design of these hybrid ligands is clearly effective since we have been able to generate a new family of group 4B derivatives that contain phosphine ligands. Although the particular hybrid ligands described here are capable of tridentate coordination, we observe only a bidentate mode of chelation both in solution and in the solid state; presumably, steric effects are the major factor in this behavior.

All of the zirconium and hafnium complexes are chiral as evidenced by solution ^1H NMR and the solid-state single-crystal X-ray structure of **4b**. This particular type of chirality is a result of the cis silylamide ligands interacting as two constrained, *geared* molecular propellers.[26] Without the chelating phosphine to constrain each molecular propeller, gear slipping[27] would occur, resulting in stereoisomerization; the ^1H NMR indicates diastereotopic nuclei up to 60 °C (>60 °C results in decomposition), thus providing additional evidence for the robust nature of the metal–phosphine linkage.

Acknowledgment. Financial support for this research was generously provided by the Department of Chemistry, the Natural, Applied and Health Sciences Fund (UBC), and the Natural Sciences and Engineering Research Council of Canada. Computing funds were provided for by Xerox Corp. and the UBC Computing Centre.

Registry No. **4a**, 84173-97-7; **4b**, 84173-98-8; **5a**, 84192-51-8; **5b**, 84236-32-8.

Supplementary Material Available: Listings of calculated coordinates and thermal parameters for hydrogen atoms (Table III), anisotropic thermal parameters (Table IV), observed and calculated structure factor amplitudes (Table V), and torsion angles (Table IX) (43 pages). Ordering information is given on any current masthead page.

(26) Mislow, K. *Acc. Chem. Res.* **1976**, *9*, 26.
(27) Johnson, C. A.; Guenzi, A.; Mislow, K. *J. Am. Chem. Soc.* **1981**, *103*, 6240.

Contribution from the Department of Chemistry, Texas A&M University, College Station, Texas 77843

An Unusual Ditantalum (Ta=Ta) Compound with a Bridging Oxo Ligand

F. ALBERT COTTON* and WIESLAW J. ROTH

Received June 21, 1982

As a minor product in the preparation of $Ta_2Cl_6(dmpe)_2$ a compound of composition $Ta_2Cl_4(dmpe)_2(\mu\text{-}O)(\mu\text{-}Me_2S)\cdot HCl\cdot C_6H_5CH_3$ has been isolated and structurally characterized. It consists of two distorted $TaCl_2P_2OS$ octahedra sharing an edge defined by the μ-Me_2S and μ-O ligands. The μ-O ligand is strongly hydrogen bonded to a Cl atom, O···Cl = 2.893 (7) Å, which may alternatively be formulated as O···H–Cl or O–H···Cl. The Ta–Ta distance of 2.726 (1) Å, together with the fact that the tantalum atoms are formally Ta^{III} (d^2), implies the presence of a double bond between the metal atoms. This compound presumably arises because of hydrolysis by traces of water coupled with the availability of the $(CH_3)_2S$ ligand, which was present in the starting material, $Ta_2Cl_6(Me_2S)_3$. The compound crystallizes in space group $P2_1/c$ with a = 14.159 (2) Å, b = 12.487 (3) Å, c = 21.174 (3) Å, β = 108.95 (2)°, V = 3540 (2) Å^3, and Z = 4.

Introduction

As part of our continuing studies on the chemistry of niobium and tantalum in their III oxidation states, we recently reported[1] the preparation of $Ta_2Cl_6(dmpe)_2$, a molecule whose structure consists of two octahedra sharing an edge and united by a Ta=Ta (double) bond, of length 2.710 (1) Å. This compound was obtained in 85% yield by the reaction of $Ta_2Cl_6(SMe_2)_3$[2] with bis(dimethylphosphino)ethane, dmpe, in CH_2Cl_2. We have now found that by appropriate workup of the mother liquor a very small amount of another binulcear tantalum(III) compound can be obtained. In this paper we report the identification and structural characterization of that compound by X-ray crystallography.

Experimental Procedures

Preparation. All manipulations were performed under an atmosphere of argon. $Ta_2Cl_6(SMe_2)_3$ was prepared according to the literature method.[2] Dmpe was purchased from Strem Chemicals, Inc., and used without further purification as a 10% w/v solution in toluene.

The title compound is a minor product obtained during the preparation of $Ta_2Cl_6(dmpe)_2$. A 1-mL quantity of the toluene solution of dmpe (0.1 g) was added to 100 mg of $Ta_2Cl_6(SMe_2)_3$ in 10 mL of CH_2Cl_2. After several hours of stirring a precipitate (accounting for ca. 85% of Ta) of red $Ta_2Cl_6(dmpe)_2$,[1] an unidentified white solid and a dark green solution were obtained. The solution was filtered and evaporated nearly to dryness. The residue was redissolved in a mixture of 5 mL of toluene and 2 mL of CH_2Cl_2, and the solution was filtered into a Schlenk tube and carefully layered with 10 mL of hexane. Upon slow diffusion of hexane into the solution layer, about 10 mg of dark green, plate-shaped crystals was formed.

X-ray Crystallography. A crystal of approximate dimensions 0.4 × 0.3 × 0.15 mm was mounted in a glass capillary with the use of epoxy cement. Unit cell parameters and intensity data were obtained on an Enraf-Nonius CAD-4 diffractometer by using standard procedures.[3] The summary of crystallographic data is presented in Table I. Polarization, Lorentz, and absorption corrections were applied to the intensity data.

Structure Solution and Refinement.[4] Positions of the two Ta atoms were obtained from a three-dimensional Patterson function. Three cycles of isotropic least-squares refinement gave values of R_1 = 0.25 and R_2 = 0.34. Subsequent series of Fourier syntheses and isotropic least-squares refinements revealed the positions of 27 non-hydrogen atoms, namely, the $Ta_2Cl_4(dmpe)_2(SMe_2)O$ molecule and a separate Cl atom. The values of R_1 and R_2 at that point were equal to 0.076 and 0.105, respectively. Following anisotropic least-squares refinement a difference Fourier map was obtained, showing 14 peaks, which were interpreted as two poorly defined toluene molecules. The refinement

(1) Cotton, F. A.; Falvello, L. R.; Najjar, R. C. *Inorg. Chem.* **1983**, *22*, 375.
(2) Cotton, F. A.; Najjar, R. C. *Inorg. Chem.* **1981**, *20*, 2716.
(3) Bino, A.; Cotton, F. A.; Fanwick, P. E. *Inorg. Chem.* **1979**, *18*, 3558.
(4) All crystallographic computing was performed on a PDP 11/60 computer at B. A. Frenz and Associates, Inc., College Station, TX, equipped with a modified version of the Enraf-Nonius structure determination package.

0020-1669/83/1322-0868$01.50/0